Vibrational Mixing and Energy Flow in Polyatomics: Quantitative Prediction Using Local Random Matrix Theory

David M. Leitner and Peter G. Wolynes*

Department of Chemistry, University of Illinois, Urbana, Illinois 61801

Received: June 27, 1996; In Final Form: October 11, 1996[⊗]

The theory of local random matrix models has provided a way for understanding many aspects of quantum ergodicity and energy flow in molecules. In this paper quantitative results are presented for a random matrix model that yields analytical expressions for the degree of vibrational mixing and flow rates in polyatomics in terms of a small number of parameters. The results of these generally applicable expressions are compared with large scale computation on energy flow in several organic molecules studied experimentally: formaldehyde, thiophosgene, and propyne. We show these systems are respectively below, at, and significantly above the quantum ergodicity transition. Effects of finite molecular size on the quantum ergodicity transition are also discussed.

I. Introduction

The central role of intramolecular energy flow in chemical kinetics and photochemistry has long motivated experimental,[1] computational,[2−4] and theoretical studies[5] of vibrational relaxation in polyatomics. Large scale simulations and experimental studies on a number of small molecules have provided a wealth of detailed information about vibrational mixing and energy transfer. However, despite notable successes on rather large molecules,[2−4] detailed analysis of the complete vibrational Hamiltonian of a large polyatomic is still a very demanding undertaking. Fortunately, such large scale computation is apparently not needed for understanding a great deal about the qualitative nature of intramolecular energy flow or, as we shall show here, even to predict the extent and rates of flow to modest accuracy. Alternative approaches[6,7] to large scale computation treat the oscillator energies and local couplings statistically, the distributions of which are parametrized to suit the harmonic vibrational spectrum and anharmonicities of a particular polyatomic. The resulting local random matrix ensemble yields analytical expressions predicting vibrational mixing, rates of energy flow, and the location of the quantum ergodicity transition between localized and extended states.

In this article, we compare predictions for vibrational energy flow and localization obtained from local random matrix models with results of computational studies[4,8,9] on several organic molecules. Our results are in some sense meant to serve as an illustration of a general approach for analyzing specific systems. The systems chosen were those for which appropriate data for comparison could be found in the literature. The molecules we consider are formaldehyde, propyne, and thiophosgene, which serve as examples of how to analyze both vibrational mixing on the localized side and flow rates on the extended side of the transition, as well as behavior near the transition. The formaldehyde molecule has long been the subject of extensive experimental analysis,[10] and recent computational studies provide additional results against which predictions of the analytical theory can be compared. Formaldehyde is also interesting because the polyad quantum number is approximately conserved at low to moderate energies,[8,11] so that a more elaborate counting scheme than that otherwise adopted[12] is required to determine local level densities for the matrix model. This special treatment, which is detailed in the Appendix, may be useful in other cases where the polyad number is approximately conserved.[13] Finally, because the local random matrix predictions strictly apply in the thermodynamic limit, it is necessary to consider effects of finite size when making predictions about a specific molecule. We examine the extent to which finite size effects lead to the possibility of large scale but not necessarily ergodic flow over the energetically available state space for some states strictly below the quantum ergodicity transition. The probability of such extensive flow is seen to decrease rapidly as the size of the molecule considered increases.

The organization of this article is as follows: The local random matrix model and its predictions for the location of the transition and for vibrational mixing and energy flow rates are summarized from previous work in section II. In section III we examine a case very convenient for describing polyatomics, a 2:1 oscillator model, where a fraction of the oscillator frequencies are about twice those of the others. Here we compare predictions for vibrational mixing with computational results[8] for formaldehyde. In section IV we compare rates of flow with numerical results for propyne,[4] which is well above its transition, and thiophosgene,[9] which is near its ergodicity transition. Finite size effects on the quantum ergodicity transition are discussed in section V.

IIA. Model

We consider a local random matrix model of the vibrational Hamiltonian $H = H_0 + V$,

$$H_0 = \sum_{\alpha=1}^{N} \epsilon_\alpha(\hat{n}_\alpha) \tag{2.1a}$$

$$V = \sum_{\mathbf{m}} \prod_{\alpha} \Phi_{\mathbf{m}} b_\alpha^{\dagger m_\alpha^+} b_\alpha^{m_\alpha^-} \tag{2.1b}$$

where $\mathbf{m} = \{m_1^{\pm}, m_2^{\pm}, ...\}$. The zero-order Hamiltonian H_0 consists of a sum over the energies of the nonlinear oscillators, where each oscillator has frequency $\omega_\alpha(n_\alpha) = \hbar^{-1}\partial\epsilon_\alpha(n_\alpha)/\partial n_\alpha$, and nonlinearity, $\omega'_\alpha(n_\alpha) = \hbar^{-1}\partial\omega_\alpha(n_\alpha)/\partial n_\alpha$, and the number operator is defined by $\hat{n}_\alpha = b_\alpha^\dagger b_\alpha$. The set of zero-order energies $\{\epsilon_\alpha\}$, and coupling terms in H, $\{\Phi_{\boldsymbol{m}}\}$, are treated as random variables. The Hamiltonian of eq 2.1 includes direct resonant coupling terms of arbitrary order. Such high-order

[⊗] Abstract published in *Advance ACS Abstracts,* December 15, 1996.

S1089-5639(96)01908-1 CCC: $14.00

terms are in general crucial in locating the transition between localized and extended states.[12,14] Defining $p = \sum_\alpha (m_\alpha^+ + m_\alpha^-)$, we assume that the $\{\Phi_\mathbf{m}\}$ decay exponentially with p as[4,15−17]

$$\Phi_\mathbf{m} = \Phi_3 \sigma^{3-p} \quad (p \geq 3) \tag{2.2}$$

where Φ_3 is a cubic coupling term. In a given molecule, Φ_3 can take on values of the order $0.1-10$ cm^{-1}; realistic values of σ typically range between 3 and 10.[4] A good approximation to the off-diagonal matrix elements of H keeps only the largest contributions generated by the coupling of eqs 2.1b and 2.2. Defining the distance $Q = \sum_\alpha |n'_\alpha - n_\alpha|$ in quantum number space, where n_α is the number of quanta in mode α of one state and n'_α the number of quanta in the same mode of the other, matrix elements connecting two states a distance Q from one another are approximated by

$$V_Q = \Phi_3 \sigma^{3-Q} M^{Q/2}, \quad Q \geq 3 \tag{2.3a}$$

$$V_Q = \Phi_3 \sigma^{1-Q} M^{Q/2+1}, \quad Q < 3 \tag{2.3b}$$

where M is the average number of quanta per mode. Equation 2.3 approximates V_Q to highest order in σ. While we neglect them here, contributions of terms lower order in σ have been evaluated in ref 17. The approximation to V_Q given by (2.3b) follows from eq 2.2, since the lowest order contributions to V_1 and V_2 come from cubic and quartic terms, respectively, so that $V_1 \sim V_3$ and $V_2 \sim V_4$. Because of large variation in Φ_3 and σ for a given molecule, we expect a large dispersion in V_Q for any Q. Nevertheless, as we shall see below, coupling matrix elements enter into theoretical preditions for vibrational mixing and flow rates only as averages. The vibrational Hamiltonian H is thus parametrized by sets of frequencies $\{\omega_\alpha\}$, nonlinearities $\{\omega'_\alpha\}$, cubic coupling terms $\{\Phi_3\}$; M, the number of quanta per mode; and σ, the rate of exponential decrease of higher order coupling terms.

IIB. Local Random Matrix Predictions

Analysis of the Hamiltonian introduced in section IIA has led to many predictions relevant to vibrational mixing and flow, details of which are provided in refs 7, 12, and 18. The aim of the analysis was to determine self-consistently rates of energy flow out of a state $|j\rangle$ of the vibrational space, an eigenstate of the uncoupled oscillator Hamiltonian H_0. Because the couplings to other states of the vibrational space defined in section IIA depend on the distance Q from $|j\rangle$ in quantum number space, the state space is organized into tiers of states, where the location of each tier corresponds to its distance Q from $|j\rangle$. We have assumed in our treatment a statistically homogeneous structure for the vibrational space; i.e., statistically, the couplings and local densities of states coupled to states of one tier are equivalent to those coupled to states of any other tier if each of the states is close in energy. The approximation of a homogeneous structure should be valid for most states of the vibrational space that are close in energy, so long as all that energy is not concentrated into one or very few of the vibrational modes. States where energy is concentrated in very few modes lie at the edge of the vibrational space. For such "edge" states, flow often proceeds through a sequence of statistically inhomogeneous tiers to the interior, due to a sparsity of flow pathways for flow from the edge. We have recently treated the problem for flow out of edge states in a model oscillator system.[14] Here we focus mostly but not exclusively on vibrational mixing and energy flow over the vast majority of states of the vibrational space that occupy the interior. Whether or not we obtain a nonzero flow rate in the self-consistent analysis depends on the local coupling and the local densities of states coupled to $|j\rangle$. This information is contained in a single parameter, T, which is defined by eq 2.4. For values of T less than 1, the self-consisent theory yields a vanishing flow rate, while finite flow rates are found for $T > 1$. The quantum ergodicity transition thus lies at the critical value $T = 1$. In addition to the location of the quantum ergodicity transition separating localized from extended states, the degree of vibrational mixing on the localized side of the transition, and rates of energy flow on the extended side are all given by analytical expressions derived from the model, each of which is determined by a few parameters characterizing the spectral dispersion and anharmonicities of the particular polyatomic studied. In this subsection we review results previously obtained[7,12,18] for the local random matrix model of H.

The central parameter determining the extent of vibrational mixing is the transition parameter, defined as

$$T(E) \equiv (2\pi/3)\left(\sum_Q K_Q \langle|\psi_Q|\rangle D_Q(E)\right)^2 \tag{2.4}$$

The transition parameter is expressed in terms of the average effective coupling, $\langle|\psi_Q|\rangle$, to states a distance Q away. The effective coupling defined by eq 2.10 incorporates both the direct coupling V_Q to these states and off-resonant contributions. If we choose to neglect the latter, then $\psi_Q = V_Q$ given by eq 2.3. Apart from the local effective coupling, the local level density is required to determine the transition parameter. The local density of states that lie a distance Q away is $K_Q D_Q(E)$, where K_Q is the connectivity and $D_Q(E)$ is the probability of there being a state at energy E. Each parameter will be determined below for oscillator systems characteristic of moderate size to large polyatomics. The sum in eq 2.4 refers to direct coupling to all sets of states a distance Q in quantum number space from the initial state.

According to the self-consistent theory, the transition between localized and extended states is found where $T(E) = 1$. When $T(E) < 1$, states are localized. The degree of localization is quantified by the inverse participation ratio,[19] y, also called the dilution factor, used by molecular spectroscopists as a measure of vibrational mixing.[20,21] The dilution factor is defined as $y = \sum_\lambda |c_{j\lambda}|^4$, where $c_{j\lambda} = \langle\lambda|j\rangle$, with $|j\rangle$ an eigenstate of H_0 and $|\lambda\rangle$ an eigenstate of the coupled oscillator Hamiltonian H. The dilution factor y is equivalently the long-time survival probability of state $|j\rangle$ and is determined experimentally by the sum of the squares of the relative intensities of the spectrum. We have shown[18] that a close approximation to the distribution of y can be expressed in terms of $T(E)$ as

$$P_y(y) = \gamma y^{-1/2}(1-y)^{-3/2} \exp\left(-\frac{\pi\gamma^2 y}{1-y}\right) \tag{2.5a}$$

$$\gamma = \left(\frac{3}{2\pi}\frac{T(E)}{1-T(E)}\right)^{1/2} \tag{2.5b}$$

A number of studies on the approach to strongly mixed or extended vibrational states consider the average dilution factor, $\langle y\rangle$, given by

$$\langle y\rangle = \int_0^1 y P_y(y)\, dy = e^{\pi\gamma^2/2} D_{-2}(\sqrt{2\pi\gamma^2}) \tag{2.6}$$

where D_p is the parabolic cylinder function. Recent numerical studies by Bigwood and Gruebele on a local random matrix model of thiophosgene[9,22] support the validity of eq 2.5 for the dilution factor distribution.

When $T(E)$ is greater than 1, eigenstates of H at energy E are extended, enabling facile energy flow throughout the vibrational state space. The theory predicts a singular critical behavior for the flow rates very near the transition. Above the transition region, an estimate for the rate, $k(E)$, of flow out of a typical state of H at energy E is given by[12]

$$k(E) = 2\pi\hbar^{-1}\sum_Q K_Q\langle|\psi_Q{}^2|\rangle D_Q(E) \qquad (2.7)$$

where eq 2.7 is the average renormalized golden rule estimate for the rate. A related but not identical result for the damping rate of an excited mode coupled to a bath of oscillators has been given by Stuchebrukhov[23] (see also ref 24).

Equation 2.7 must be distinguished from the usual golden rule expression, for which $D_Q(E)$ is replaced by the zero-order density. This distinction becomes most apparent at high coupling, where $D_Q(E)$ varies inversely with the coupling (cf. eq 2.8); for large couplings the energy flow rate then varies linearly with coupling rather than quadratically.[7,12] In fact, linear variation of flow rates with large coupling is only one feature of vibrational energy flow in polyatomics that departs from the traditional assumptions. Schofield and Wolynes[25] have argued that the locality of couplings allows enhanced returns to the initial state so that the survival probability decays in local random matrix models as a power law rather than exponentially at long times. Several computational studies have reported such power law decays and linear rate dependence with coupling.[4,9,26]

In order to estimate the extent of vibrational mixing or rates of flow, we need to determine the values of three parameters as a function of the distance Q in quantum number space: the effective coupling, ψ_Q; the connectivity K_Q; and the local density of states D_Q. An analytical expression for D_Q is obtained assuming that the distribution of states of H_0, the uncoupled oscillator Hamiltonian, a distance Q from a given state is described by a Lorentzian distribution with a width characteristic of the dispersion in oscillator frequencies. In this way an approximation to $D_Q(E)$[12] is found to be

$$D_Q(E{=}\epsilon_j) = \frac{2}{\pi[\lambda_Q + (\lambda_Q{}^2 + 4\sum_Q K_Q\bar{V}_Q{}^2)^{1/2}]} \qquad (2.8)$$

where $\bar{V}_Q$ is the typical, or average, value of V_Q. The width λ_Q depends on the oscillator frequencies, which we represent with the root-mean-square, $\omega_{\rm rms}$, of the set of oscillator frequencies, $\{\omega_\alpha\}$, and should grow with Q as $Q^{1/2}$, so we set $\lambda_Q = Q^{1/2}\hbar\omega_{\rm rms}$. Below and near the transition $D_Q(E{=}\epsilon_j)$ can be adequately approximated as ($\hbar = 1$)

$$D_Q(E{=}\epsilon_j) \approx (\pi Q^{1/2}\omega_{\rm rms})^{-1} \qquad (2.9)$$

which is just the zero-order density. Comparing eqs 2.4 and 2.8, we observe that eq 2.9 is reasonable for values of $\bar{V}_Q$ satisfying $\bar{V}_Q \lesssim K_Q{}^{1/2}\bar{V}_{Q,c}$, where $\bar{V}_{Q,c}$ is the value of $\bar{V}_Q$ at the transition. For larger values of $\bar{V}_Q$, $D(E)$ varies inversely with $\sum_Q K_Q\bar{V}_Q{}^2$, whereby rates vary linearly with coupling.

The effective coupling ψ_Q can in many cases be approximated by the direct coupling V_Q given by eq 2.3. However, at low energies off-resonant contributions can modify $T(E)$ significantly. A mean-field treatment of off-resonant terms adopted in determining ψ_Q is given in ref 12. The result can be most conveniently represented diagrammatically[27] as follows:

$\psi_{Q,jk} =$ 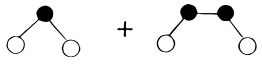 $\cdots$ (2.10)

The interpretation of each diagram, which from left to right represents terms of successively higher order, is as follows: Each segment of any diagram is associated with $\langle V_q\rangle$ and each filled vertex with $K_q\langle(\Delta E_q)^{-1}\rangle$, where ΔE_q is the level spacing to states a distance q from the previous vertex. A sum over q at each filled vertex, under the constraint that the total quantum number change is Q, is implicit in each diagram. The first diagram, then, represents direct coupling between two states and is assigned the value V_Q. The second term involves a transition via one intermediate state and represents $\sum_q\langle V_q\rangle\langle(\Delta E_q)^{-1}\rangle\langle V_{q'}\rangle$, where $q + q' = Q$ or $|q - q'| = Q$. We note that in the extended domain and when couplings become large, all diagrams but the first one provide only very small contributions to ψ_Q, since, just like D_q above, $\langle(\Delta E_q)^{-1}\rangle$ becomes smaller with $|V_q|$. A reasonable estimate for $\langle(\Delta E_q)^{-1}\rangle$ is to use the average of the inverse spacing of the uncoupled intermediate states when $V_Q \lesssim K_Q{}^{1/2}V_{Q,c}$. When the coupling is large enough such that $V_Q \gtrsim K_Q{}^{1/2}V_{Q,c}$, one can set $\langle(\Delta E_q)^{-1}\rangle \sim (\sum_q K_q{}^{1/2}|V_q|)^{-1}$, and the high-order terms can be thereby neglected.

The connectivity K_Q to states a distance Q away is easily estimated for a large number N of coupled oscillators. An adequate estimate for K_Q has been derived in ref 12 and is given by

$$K_Q \approx (2N)^Q/Q! \qquad (2.11)$$

when N is large and Q is less than $\approx 2N^{1/2}$, which is generally sufficient for locating $T(E)$ and estimating flow rates. If there are any selection rules that would modify the number of accessible states, a more specific counting procedure is required to estimate K_Q. In the following section we treat an example where the polyad quantum number is approximately conserved.

III. Vibrational Mixing among 2:1 Oscillators

In this section we examine a particular realization of the model described in section II. We consider a system of N coupled nonlinear oscillators, where N_1 of the N oscillators have frequencies with average $\bar{\omega}_1$, while the average of the $N_2 = N - N_1$ other oscillator frequencies is $\bar{\omega}_2$, where $\bar{\omega}_2 \approx 2\bar{\omega}_1$ over the range of energy we consider. Because of the 2:1 resonance structure, the polyad quantum number N_t is approximately conserved over these energies. For a 2:1 oscillator system the polyad number is given by $N_t = q_1N_1 + 2q_2N_2$, where q_1 (q_2) is the total number of quanta among the N_1 (N_2) oscillators. This particular oscillator system mimics certain polyatomics in significant respects. Often stretch:bend frequency ratios are approximately 2:1; a particular example is formaldehyde, where each of $N_1 = 4$ modes has frequency $\approx$1500 cm^{-1}, while the frequencies of the other two modes are about 3000 cm^{-1}. We consider formaldehyde in more detail below.

We begin by determining the location of the transition between localized and extended states in this 2:1 oscillator system. For this we need to compute $T(E)$ using eq 2.4, which requires information about the coupling incorporated in ψ_Q, the connectivity K_Q, and local level density $D_Q(E)$ of states that lie a distance Q from a given excited state. To lowest order in the coupling, $\psi_Q = V_Q$ given by eq 2.3; to compute higher order terms, information is required about the connectivities to states participating in off-resonant transitions between the initial and final states.

To determine K_Q, we need first to estimate the number of quanta in each mode, broken down into the number of quanta in each of the N_2 oscillators with frequency $\approx\bar{\omega}_2$, and in each of the remaining N_1 oscillators. With this information the number of ways to remove quanta from the oscillators for a given polyad quantum number N_t can be calculated; then the

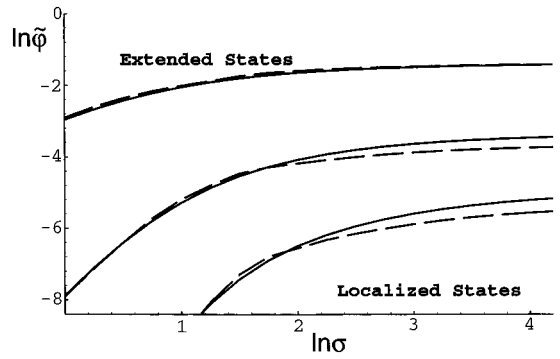

Figure 1. Transition curves separating localized from extended regions for 2:1 oscillator systems, where the ratio of N_1 to N_2 is 2:1. The total number of oscillators is, from top to bottom, $N = 6$, 18, and 48 oscillators; the polyad number is $N_t = 8$. Plotted is ln $\tilde{\phi}$, where $\tilde{\phi} \equiv \Phi_3 M^{3/2} \omega_{\text{rms}}{}^{-1}$ is the scaled cubic coupling, and ln σ, where σ is the exponential decrease in magnitude of higher order resonant coupling terms. Solid curves represent estimates for $T(E) = 1$ when $\psi_Q = V_Q$, and dashed curves locate the transition when ψ_Q is computed using the two lowest order terms of eq 2.11.

combination of ways to move a distance Q in quantum number space while conserving N_t is counted. This calculation would be sufficient for determining $T(E)$ if we approximated ψ_Q by the first term in eq 2.10. However, for the other terms, we also need to count the number of ways to make off-resonant transitions, so that the connectivity to values of higher and lower N_t must also be determined. Details of the calculation of K_Q are provided in the Appendix.

In Figure 1 we illustrate results comparing the location of the transition using eq 2.4 when first- and second-order terms in ψ_Q are present, with those where $\psi_Q = V_Q$. For several cases we plot ln $\tilde{\phi} \equiv \ln(\Phi_3 M^{3/2} \omega_{\text{rms}}{}^{-1})$, where $\tilde{\phi}$ is the scaled cubic coupling, versus ln σ at their critical values corresponding to the quantum ergodicity transition at $T = 1$. The oscillator frequencies have been fit to those of formaldehyde,[8] where $\bar{\omega}_1 = 1445$ cm^{-1}, $\bar{\omega}_2 = 2975$ cm^{-1}, and $\omega_{\text{rms}} = 192$ cm^{-1}. The number of modes is $N = 6$ (formaldehyde), 18, and 48; the ratio of N_1 to N_2 is 2:1; and the polyad number is $N_t = 8$. Figure 1 illustrates the role of off-resonant terms in locating the quantum ergodicity transition using parameters representative of organic molecules. We observe in the figure that the role of higher order terms in eq 2.10 becomes more significant as the ratio N:N_t increases, which reflects the greater role of off-resonant terms when the number of quanta per mode becomes small. This trend is not unexpected, since the inverse level spacing $\langle(\Delta E_q)^{-1}\rangle$ of off-resonant states contributes to all terms in ψ_Q except the first one. Due to sign cancellation $\langle(\Delta E_q)^{-1}\rangle$ will generally be small unless the total energy is very low, since only at very low energy are there more off-resonant levels of higher energy that are not canceled by those lower in energy. We moreover observe the effect of higher order terms to be most significant for large σ, which is consistent with our expectation that small σ favors direct exchange, while large σ makes vibrational superexchange a possible energy flow mechanism.[14] We mention that the results presented in Figure 1 do not change much upon changing the ratio of N_1:N_2. However, the results are quite different in the absence of 2:1 resonances. In the case where only 1:1 resonances are available, higher order terms in eq 2.10 are required for saturation of the transition curves with large σ.[14]

We are finally in a position to make direct comparisons with results for formaldehyde. Sibert and co-workers[8,11] computed average values of the participation numbers for formaldehyde for polyad numbers up to 8 ($\approx$12 000 cm^{-1}) with a detailed potential model. They went on to study also a random matrix model mimicking the vibrational Hamiltonian of formaldehyde

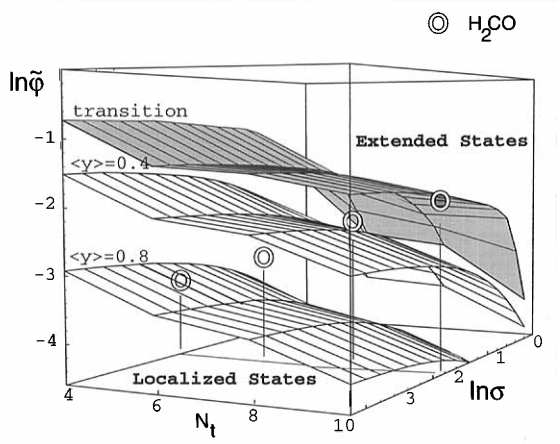

Figure 2. Surfaces representing, from top to bottom, values of $\tilde{\phi}$, σ, and N_t when the average dilution factor $\langle y\rangle = 0$ (the transition), 0.4, and 0.8, for a 2:1 oscillator system where $N_1 = 4$ and $N_2 = 2$. $\tilde{\phi}$ is the scaled cubic coupling, and σ is the exponential decrease in magnitude of high-order resonant coupling terms. N_t is the polyad number defined by $N_t = q_1 N_1 + 2q_2 N_2$, where q_1 (q_2) is the total number of quanta among the N_1 (N_2) oscillators. Using representative values for formaldehyde,[8] values of $\langle y\rangle$ are found to be 0.83, 0.55, 0.30, and 0.05 respectively at polyad numbers $N_t = 4$, 6, 8, and 10, indicated by the circles in the figure. The vertical gray lines have been drawn in for orientation. Note that curves connecting the integral values of N_t are only a guide.

as part of a more general study of rotation−vibration mixing in formaldehyde, finding very close agreement between the participation numbers obtained from their formaldehyde Hamiltonian and the corresponding matrix ensemble. We now compare results of ref 8 for the average participation number, with the inverse of the average dilution factor predicted by eq 2.6, bearing in mind that these two averages are not identical. In our case, we can simply insert representative values for formaldehyde by adopting a 2:1 system where $N_1 = 4$ and $N_2 = 2$. Formaldehyde at a given polyad number N_t then appears as a point on a plot like Figure 1. If we plot the same parameters, $\tilde{\phi}$ and σ, as in Figure 1 at several values of the polyad number N_t, we can observe how formaldehyde approaches the ergodicity transition with N_t. Such a plot is presented in Figure 2. Each surface in the figure corresponds, from top to bottom, to successively larger values of the average dilution factor, $\langle y\rangle$, in the range 0 (the transition) to 1, and therefore to smaller values of $T(E)$ (cf. eq 2.6). The positions of formaldehyde in the figure were determined by using $\Phi_3 = 15.2$ cm^{-1}, which we have estimated from the data in ref 8, using $M = 0.9$ for $N_t = 6$, and by setting $\sigma = 10$, which implies that cubic terms essentially locate the transition in the simulated random matrix model.[30] For example, the value of T obtained at $N_t = 8$ is 0.31, and from eq 2.6, we find a value of $\langle y\rangle = 0.30$ for the average dilution factor. This compares well with 0.11, the value of the inverse of the average participation number at $N_t = 6$ obtained in ref 8. At $N_t = 4$ and 6, we find T for formaldehyde to be 0.01 and 0.08, respectively, yielding 0.83 and 0.55 for the average dilution factors, respectively. These can be compared with 0.56 and 0.23, respectively, the inverse of the average participation numbers reported in ref 8, where again we find quite reasonable agreement. We moreover estimate that $T \approx 1$ when $N_t = 10$, as seen in Figure 2, so that for polyad numbers larger than 10 vibrational energy flow in formaldehyde is predicted to be global.

It is worthwhile pointing out that reasonably similar results for T are obtained even if information about connectivities to sets of oscillators with different values of the polyad quantum number is neglected. If we admit coupling to all states a distance Q away, regardless of their value of N_t, then eq 2.11 can be used to estimate the connectivity. Then using eq 2.9

for the local density of states, where now ω_{rms} is the root-mean-square frequency of all the oscillators, we find $T = 0.48$ for $N_t = 6$, giving an average dilution factor of 0.20; while $T = 1.2$ when $N_t = 8$, suggesting energy flow in this polyad would be already largely ergodic if we could ignore the polyadic constraint.

IV. Polyatomic Molecules

The case of formaldehyde illustrates how the theory can be applied when an approximately conserved quantity, the polyad quantum number, is explicitly treated. The constraint of polyad numbers enters into estimates for the local level densities, for which a special counting procedure was adopted. This may be easily generalized to other cases when faced with similar selection rules. For many moderate size organic molecules (or other polyatomics generally) a simpler approach to determining the local level density is possible, whereby the connectivity K_Q can be estimated directly from eq 2.11. In the following, we use the simpler approach to estimate rates of vibrational energy flow in two examples, propyne and thiophosgene. These systems have been studied computationally by Gruebele and co-workers,[4,9] so we can study the analytic results without concern about modeling the energy surface. We assume throughout that the states from which energy flow commences are typical, since as discussed in section IIB action space is not entirely homogeneous, in particular near the edge of the vibrational space. While flow out of all coupled states at energy E is predicted to be global when the transition parameter $T(E)$ is greater than 1,[14] rates of flow out of special states may not be typical. Flow out of edge states, where excitation is located in only one or very few modes, is in particular not expected to exhibit flow rates that are typical of those of most isoenergetic "interior" states due to the sparsity of flow pathways following excitation.[1−3] This leads to a specific pathway mechanism often involving dynamical tunneling.[3,28] These edge states are in many cases the easiest to interrogate experimentally so they have received considerable attention in the laboratory.

Our first example is propyne, which has been the subject of intensive experimental[29,31,32] and computational[4,33] investigation. Laboratory experiments show that the second overtone of the acetylenic CH stretch ($3\nu_1$) decays at a rate of about 3 ns^{-1}.[32] In a computational analysis of propyne, a flow rate of $\approx$3 ns^{-1} out of the same edge state was also observed.[4] Bigwood and Gruebele moreover computed energy flow rates for a number of isoenergetic interior states, finding that flow out of interior states at this energy of about 9700 cm^{-1} is considerably faster than flow out of the acetylenic stretch. In particular, Bigwood and Gruebele's computations revealed an average flow rate of $k \approx 1.5$ ps^{-1} over 20 interior states.

To estimate flow rates for propyne using the results summarized in section II, average values for the coupling terms are required. Off-diagonal anharmonicities for each mode of propyne are listed in ref 4. Bigwood and Gruebele have used as an average over all combinations of modes a value of $\bar{\Phi}_3 = 2.8$ cm^{-1}. Values of σ are seen in ref 4 to vary between 3 and 10 for the range of total energies analyzed, and as an overall average over combinations of modes we use $\sigma = 6.4$. The root-mean-square frequency of the 15 oscillators is $\omega_{rms} = 1927$ cm^{-1}, which using eq 2.8 yields an estimate for the local density of states D_Q. We assume that the coupling ψ_Q is simply given by the direct resonant coupling V_Q. Then using eq 2.11 for the connectivities, we compute the transition parameter T and flow rates using eqs 2.4 and 2.7, respectively. We find the transition paramater to be about 40 for propyne using the parameters given above, so that states with energies near 9700 cm^{-1} are indeed extended, and facile vibrational energy flow typically occurs.

TABLE 1: Estimates for the Transition Parameter, T, and Energy Flow Rates among Interior States of Propyne, Using Results of the Local Random Matrix Model Summarized in Section II[a]

energy (cm^{-1})	T	T_3	rate (ps^{-1})	rate in ref 4
3400	0.4	0.1		
6600	7	1	1.2	
9700	40	3.3	4.8	1.5

[a] T_3 is an estimate for T obtained by truncating eq 2.4 at $Q = 3$ (see text). The energies listed lie close to those of ν_1, $2\nu_1$, and $3\nu_1$.

The rate of energy flow is found to be $\approx$4.8 ps^{-1}, reasonably close to the result of about 1.5 ps^{-1} obtained by Bigwood and Gruebele in their large-scale computation.

We mention that the value for T obtained from eq 2.4 is quite sensitive to the presence of relatively high-order resonant coupling terms in the propyne Hamiltonian. For example, we could estimate T by retaining only cubic terms, which amounts to truncating eq 2.4 at $Q = 3$. This estimate for T, T_3, is then $T_3 \approx 3.3$, which is very close to the transition value of 1. The sensitivity of $T(E)$ to higher-order resonances in propyne is consistent with our previous observation concerning the general role of high-order direct resonant coupling terms in locating the ergodicity transition in large polyatomics.[12,14] Above the transition region, however, energy flow rates depend largely on low-order terms.[12] For example, in propyne near 9700 cm^{-1} we find a rate of 3.4 ps^{-1} using only cubic terms, which is not very different from our predicted rate with high-order terms included. The important contribution of high-order resonances to flow rates enters in only at higher energies.

Spectroscopic studies suggest that the treshold to energy flow in propyne should lie at an energy not very much below $3\nu_1$.[31,32] Energy flow out of the $2\nu_1$ state is at best very much slower; in the absence of Coriolis coupling the $2\nu_1$ propyne spectrum reveals no vibrational relaxation. Whether or not energy can flow out of the $2\nu_1$ state to states of the interior depends on whether the isoenergetic interior states are extended or localized. One recent computational study of propyne suggests there is no flow to the interior,[33] though this study adopted only low-order resonant coupling terms in the Hamiltonian, and we have seen that the existence of extended states rests to a large extent on higher order resonances. We can use eq 2.4 to estimate the value of $T(E \approx 6600$ cm$^{-1})$ for propyne. We adopt again the propyne parameters provided in ref 4 and adjust M, the average number of quanta per mode, for propyne at around 6600 cm^{-1} to be about two-thirds its value for propyne near 9700 cm^{-1}. We thereby obtain estimates for the coupling matrix elements using eq 2.3. We then find for the transition parameter at energies near $2\nu_2$ a value of $T \approx 7.0$, which lies above though reasonably close to the ergodicity transition. This estimate for T is also sensitive to high-order resonances, as we find T_3, the estimate for T obtained by retaining only cubic terms, to be just below 1.

We conclude that the ergodicity transition in propyne lies at an energy very near that of $2\nu_1$. Still, even if the interior states of propyne near 6600 cm^{-1} are extended as the value $T \approx 7$ suggests, flow to the interior would still be very slow due to the sparsity of pathways to reach the interior. We recall that such sparsity is responsible for the 3 order of magnitude difference in rates between flow out of the $3\nu_1$ edge state and the isoenergetic interior states. We may well have differences of this order or more for flow out of the $2\nu_1$ state, and the isoenergetic interior states, for which we predict a rate using eq 2.7 of about 1.2 ps^{-1}. A summary of results for propyne is listed in Table 1.

Before completing our discussion of propyne, we mention one issue concerning the application of our model to larger

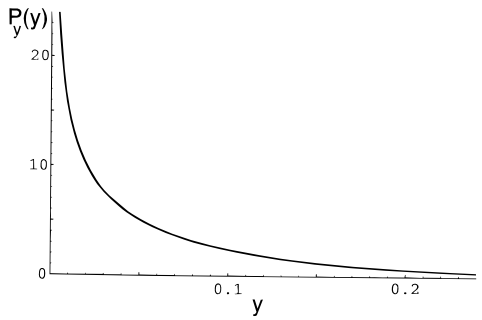

Figure 3. Distribution of the dilution factor y given by eq 2.5, when $T = 0.85$.

organic molecules. The coupling scheme presented in section IIA does not as yet distinguish between coupling of vibrational motions in different parts of the molecule with coupling of nearby vibrations, such as vibrational motion involving common atoms. Locality of vibrational motion can arise through formation of local modes,[34] which become ever more prevalent in larger organic molecules. There is even evidence for some locality in propyne, as suggested by the apparently somewhat slower relaxation out of the combination band $\nu_1 + 2\nu_6$, corresponding to CH stretches on opposite sides of propyne, as compared to nearly isoenergetic $3\nu_1$.[35] Such effects, which could be significant in larger molecules, will of course lower the connectivity now estimated by eq 2.11, thereby lowering estimates for the transition parameter $T(E)$ and energy flow rates.

A second molecule we consider in this section is thiophosgene, $SCCl_2$. Vibrational mixing and relaxation properties of thiophosgene were studied by Gruebele,[9] who numerically solved a random matrix model parametrized by couplings and frequencies representative of $SCCl_2$. We compare results of this analysis with predictions of section II. For energies around 12 000 cm^{-1} above the ground state, a characteristic cubic coupling term is $\bar{\Phi}_3 = 5$ cm^{-1}, and a representative value of σ is 6.5. The root-mean-square oscillator frequency over the six vibrational modes is 657 cm^{-1}. Putting these quantities into eqs 2.9, 2.11, and 2.4, we find for $T(E)$ a value of 0.85, which is very close to the critical value $T(E) = 1$. In fact, possible errors introduced by using crude statistical distributions (e.g., a Lorentzian to describe the zero-order local density of states) as well as systematic error in the self-consistent theory would allow thiophosgene to be either somewhat above or below the quantum ergodicity transition.

Though still below the predicted transition, we expect mixing of states in the state space to be relatively extensive when $T(E) = 0.85$. We can make this precise by considering the dilution factor distribution $P_y(y)$, given by eq 2.5, at $T = 0.85$, which we plot in Figure 3. We see in the figure that the distribution rises steeply as y approaches 0, so that many states with very small y are predicted even below the transition. Since y is equivalent to the long-time survival probability of the initially excited state, decay to small values of the survival probability would often be observed, indicating facile energy flow to a large number of states. When y is sufficiently small such that the participation number embraces the available state space, energy flow can be said to be global. For a molecule as small as $SCCl_2$, this possibility is not so improbable when $T(E) = 0.85$, as discussed in the following section. Since y is typically small, and for some states y reaches its minimum value, a meaningful rate of energy flow can still be determined even if flow is not always completely global. Using eq 2.7, we find the rate of energy flow in thiophosgene at around 12 000 cm^{-1} to be 2.8 ps^{-1}, quite close to 1.7 ps^{-1} reported in ref 9. We note also that close agreement has been observed[22] between the dilution factor distribution given by eq 2.5 and results for thiophosgene-like molecules, for which the cubic coupling is systematically varied around its representative value of 5 cm^{-1}.

V. Finite Size Considerations

The issue of finite molecular size arises in the context of the local random matrix predictions of section II, in that it imposes an ultimate limit to the extent of state space available for energy to flow. A sharp transition to global energy flow occurs strictly only when the energetically available state space is infinite. Still, we should bear in mind that the complete density of states of a moderate-size molecule is often comparable to the single-particle state density of a macroscopic sample of metal, which does show critical behavior.[36] We now consider the extent to which the picture of a crisp transition in the thermodynamic limit is modified by the finite size of the available state space. Our analysis is semiquantitative but provides an initial orientation to the problem.

We have turned to the dilution factor to provide a measure of the extent of mixing. The dilution factor is approximately the inverse of the number of states participating in energy flow and therefore vanishes at the ergodicity transition if the vibrational state space is infinite. In finite systems, the dilution factor y reaches a minimum value y_m as limited by the size of the state space. We can estimate the minimum value y_m as the product of $\rho_g(E)$, the global level density, and $\bar{k}(E)$, the average renormalized golden rule rate of eq 2.7, whereby

$$y_m = (\hbar \rho_g(E)\, \bar{k}(E))^{-1} \tag{5.1}$$

From eq 5.1 we see how y_m approaches zero as the molecule becomes larger. The average rate $\bar{k}(E)$ varies only with local couplings and the local density of states, $\rho_l(E)$, which grows as a polynomial in the number of vibrational modes N. On the other hand, ρ_g grows exponentially with N, so that y_m becomes exponentially smaller as the number of vibrational modes increases, indicating a rapid approach to a sharp transition with the size of the molecule.

We can also use eq 5.1 to estimate the range ΔT in the value of the transition parameter $T(E)$ near the thermodynamic-limit critical value $T(E) = 1$, over which the actual crossover to global energy flow in a given molecule occurs. In an infinite system there is a sharp transition at $y_m = \langle y \rangle = 0$; in a finite system there will be a crossover to global energy flow, which has been reached, say, when $y_m = \langle y \rangle$ (>0), occurring when $T(E)$ is near but not precisely at the infinite system transition value. Equation 5.1 indicates that the difference ΔT between the crossover value of $T(E)$ and the critical value $T(E) = 1$ becomes exponentially small with larger N, and the question then is how large ΔT is for a molecule as small as thiophosgene. For the thiophosgene example at ≈12 000 cm^{-1} discussed above, $\rho_g \approx 200$ cm,[9] and using the estimate for $\bar{k}$ of 2.8 ps^{-1}, we have $y_m \approx 3 \times 10^{-4}$ from eq 5.1. Taking this value for y_m, the width of the crossover to global flow where $\langle y \rangle = y_m$ is found using eq 2.6 to be $\Delta T \approx 10^{-4}$, so that the quantum ergodicity "transition" is indeed close to the thermodynamic limit for a molecule even as small as $SCCl_2$, supporting our picture of a relatively crisp transition for energy to flow globally throughout the vibrational space.

Nevertheless, it is possible to observe rather extensive energy flow in relatively small molecules over a sizable portion of the state space at values of T smaller than this crossover value of 1. This is because even when $\langle y \rangle > y_m$ there is still a finite fraction of states for which y is predicted by eq 2.5 to be less than y_m and therefore globally mixed. For thiophosgene at 12 000 cm^{-1}, for example, we predict $T(E) = 0.85$. Using eq 2.5, we find that 6% of the states lie where $y < y_m$ and almost 20% where $y < 10y_m$, which still corresponds to mixing over a

significant fraction of the available state space. The form predicted for $P_y(y)$ at $T = 0.85$ is shown in Figure 3. Since y_m gets smaller exponentially as the number of vibrational modes increases, the fraction of states for which energy flow is reasonably extensive below but near the ergodicity transition becomes very much smaller for larger molecules.

VI. Concluding Remarks

In this article we have compared analytical expressions for vibrational mixing and flow rates derived from a local random matrix model of the vibrational Hamiltonian of moderate size polyatomics, with detailed computational results for several organic molecules. The results presented above offer considerable encouragement for applying these simple random matrix predictions to energy flow among typical vibrational states of moderate size organics containing four or more atoms. Results for formaldehyde compare favorably with available data[8] on vibrational mixing. Energy flow rates predicted for propyne at about 9700 cm^{-1} above the ground state compare well with those obtained from simulations[4] of flow out of most states near that energy.

We have also addressed effects of finite molecular size on the quantum ergodicity transition. The local random matrix predictions derived thus far hold strictly in the thermodynamic limit; in finite systems, global energy flow is still possible out of a finite fraction of states below the quantum ergodicity transition, though the probability is seen to decrease rapidly with the size of the molecule. This explains the extensive energy flow out of states of thiophosgene[9,22] at energies somewhat below those at which it is predicted to be ergodic.

Acknowledgment. We are delighted to contribute this article to the Festschrift for Saburo Nagakura, who has been incredibly influential in building chemical physics in Japan and internationally. P.G.W. began to seriously pursue the study of quantum vibrational energy flow while a guest at the Institute for Molecular Science in Okazaki, where Nagakura's kind hospitality was much appreciated. We gratefully acknowledge helpful discussions with M. Gruebele and E. L. Sibert and support from NSF Grant CHE 95-30680.

Appendix

In this Appendix we describe the counting procedure for the 2:1 oscillator system discussed in section III. While the counting scheme discussed below is applicable to this specific system, it is straightforward to generalize it to any *n*:*m* oscillator system or to oscillator systems with more than two sets of oscillators.

For convenience, we define the notation $K^{(N_t)}_{\Delta N_t,Q}$, which labels the connectivity K by the polyad number of the initial state in the superscript; ΔN_t is the difference in value of the polyad quantum numbers between the final and initial states, and Q is the distance in quantum number space. To lowest order in the effective coupling ψ_Q (cf. eq 2.10), only $K^{(N_t)}_{0,Q}$ corresponding to direct resonant transitions is required. Higher order terms corresponding to a respectively larger number of off-resonant transitions require information about $K^{(N_t)}_{\Delta N_t,Q}$. We compute $K^{(N_t)}_{\Delta N_t,Q}$ averaging over all combinations of q_1 quanta of excitation among the 1-oscillators (with frequencues $\approx\bar{\omega}_1$) and q_2 quanta of excitation among the 2-oscillators, subject to the polyad constraint $N_t = q_1N_1 + 2q_2N_2$. The number of ways to arrange q_1 quanta among N_1 modes is

$$\Theta_1 = \binom{N_1 + q_1 - 1}{q_1} \tag{A1}$$

The total number of states for a given (q_1,q_2) pair is then $\Theta_1\Theta_2$.

To determine $K^{(N_t)}_{\Delta N_t,Q}$ for given values of q_1 and q_2, we must find the combination of ways to add and to remove quanta from the N_1 and N_2 oscillators. It is always possible to add quanta to the oscillators, but removing q quanta from an oscillator requires that that oscillator be already excited to at least q quanta. We have to therefore determine the probability that there are at least q quanta in any of the N_1 (N_2) oscillators, given that there are q_1 (q_2) quanta distributed among them, and this will be done below. We define $m^{(q_1)}_{1d}(q)$ ($m^{(q_2)}_{2d}(q)$) as the number of ways to remove q quanta from N_1 (N_2) oscillators when q_1 (q_2) quanta are distributed among them and $m_{1u}(q')$ ($m_{2u}(q')$) as the number of ways to add q' quanta to those of the N_1 (N_2) oscillators from which q of the q_1 (q_2) quanta available have not already been removed. We can then express $K^{(N_t)}_{\Delta N_t,Q}$ as

$$K^{(N_t)}_{\Delta N_t,Q} = \{ \sum_{\substack{a,b,c,d;\\ a+b+c+d=Q\\ (b-a)N_1+2(d-c)N_2=\Delta N_t}} m^{(q_1)}_{1d}(a)\, m_{1u}(b)\, m^{(q_2)}_{2d}(c)\, m_{2u}(d)\}_{q_1,q_2} \tag{A2}$$

where $\{\ \}$ indicates averaging over all combinations of q_1 and q_2 such that $N_t = q_1N_1 + 2q_2N_2$. Computing $K^{(N_t)}_{\Delta N_t,Q}$ is furthermore broken down to computing the products $m^{(q_1)}_{1d}(a)m_{1u}(b)$ and $m^{(q_2)}_{2d}(c)m_{2u}(d)$, which we turn to now.

To determine $m^{(q_1)}_{1d}(a)$, we need information about the number of quanta in each of the N_1 modes. We define $\bar{n}^{(q_1,\mathbf{N}_1)}_1(q)$ as the average number of oscillators among the N_1 total that are excited to q or more quanta, given that there are q_1 quanta of excitation distributed among the N_1 modes. We then find that

$$\bar{n}^{(q_1,N_1)}_1(1) = {\Theta_1}^{-1} \sum_{p=1}^{\min(q_1,N_1)} p\binom{N_1}{p}\binom{q_1-1}{p-1} \tag{A3}$$

$$\bar{n}^{(q_1,N_1)}_1(2) = {\Theta_1}^{-1} \sum_{p=1}^{\min(q_1,N_1)} \sum_{r=1}^{q_1-2p} p\binom{N_1}{p}\binom{q_1-r-p-1}{p-1} R^{(1)}_{p,r} \tag{A4a}$$

$$R^{(1)}_{p,r} = \binom{N_1-p}{r} \tag{A4b}$$

$$\bar{n}^{(q_1,N_1)}_1(m) = {\Theta_1}^{-1} \sum_{p=1}^{\min(q_1,N_1)} \sum_{r=1}^{q_1-mp} p\binom{N_1}{p}\binom{q_1-r-(m-1)p-1}{p-1} R^{(m-1)}_{p,r} \tag{A5a}$$

$$R^{(l)}_{p,r} = \sum_{i=0}\binom{N_1-p}{i} R^{(l-1)}_{p+i,r-li} \tag{A5b}$$

With information about the average number of quanta per mode, we can now compute $m^{(q_1)}_{1d}(a)m_{1u}(b)$. All possible ways to remove a quanta from N_1 oscillators must be considered: removing all a quanta from one oscillator, removing $a-1$ from one and 1 from any of the remaining $N_1 - 1$ oscillators, removing $a-2$ from one and 2 quanta from any one of the others, or 1 quantum from each of two of the remaining oscillators, etc. All of these possibilities have to be counted to determine $m^{(q_1)}_{1d}(a)m_{1u}(b)$. Let l be the number of oscillators losing at least one quantum of excitation for any one contribution; then b quanta will be added to the remaining $N_1 - l$ oscillators. For example, for the four contributions for removing a quanta listed above, $l = 1$, 2, 2, and 3, respectively.

Accounting for all the contributions to $m_{1d}^{(q_1)}(a)m_{1u}(b)$, we arrive at the following algorithm

$$m_{1d}^{(q_1)}(a)m_{1u}(b) = \sum_{i=1}^{a}\sum_{k}\binom{(N_1 - l) + b - 1}{b} \times \prod_{j=i}^{a}\binom{\bar{n}_1^{(q_1,N_1)}(a + 1 - j) - \sum_{j'=i}^{j-1} l_{j'}}{l_j} \quad \text{(A6)}$$

where $l = \sum_{j=i}^{a} l_j$. Each product of binomial coefficients is one contribution to $m_{1d}^{(q_1)}(a)m_{1u}(b)$. The first coefficient gives $m_{1u}(b)$, where the number of oscillators to which quanta can be added is $N_1 - l$. Values of l_j in eq A6 are determined as follows: For the first product of binomial coefficients, $l_{j=i}$ is given by the closest integer less than or equal to $a/(a + 1 - j)$, and $l_{j\neq i}$ is given by the closest integer less than or equal to $(a - \sum_{j'=i}^{j-1} l_{j'}(a + 1 - j'))/(a + 1 - j)$. The first product accounts for the first contribution to $m_{1d}^{(q_1)}(a)m_{1u}(b)$. The sum over k serves to change if possible any values of l_j in the products of the binomial coefficients before changing the index i in the first sum. Values of l_j are systematically lowered for all j except $j = a$, keeping $l_i \geq 1$. The lowering of l_j continues until $l_i = 1$, and all $l_{j\neq i}$ except l_a are zero. Then the index i is increased by 1, and the l_j are computed as for the first product. An identical calculation is carried out for $m_{2d}^{(q_2)}(c)m_{2u}(d)$ in order to complete eq A2.

References and Notes

(1) For reviews, see: Lehmann, K. K.; Scoles, G.; Pate, B. H. *Annu. Rev. Phys. Chem.* **1994**, *45*, 241. Felker, P.; Zewail, A. *Adv. Chem. Phys.* **1988**, *70*, 265. Parmenter, C. S. *Faraday Discuss. Chem. Soc* **1983**, *75*, 7. McDonald, J. D. *Annu. Rev. Phys. Chem.* **1979**, *30*, 29.

(2) Wyatt, R. E. *Adv. Chem. Phys.* **1989**, *73*, 231. Wyatt, R. E.; Iung, C. *J. Chem. Phys.* **1993**, *98*, 3577. Wyatt, R. E.; Iung, C. *Ibid.* **1993**, *99*, 2261.

(3) Stuchebrukhov, A. A.; Marcus, R. A. *J. Chem. Phys.* **1993**, *98*, 6044. Stuchebrukhov, A. A.; Mehta, A.; Marcus, R. A. *J. Phys. Chem.* **1993**, *97*, 12491.

(4) Bigwood, R.; Gruebele, M. *Chem. Phys. Lett.* **1995**, *235*, 604.

(5) For a review, see: Uzer, T. *Phys. Rep.* **1991**, *199*, 73.

(6) Kuzmin, M.; Stuchebrukhov, A. A. In *Laser Spectroscopy of Highly Vibrationally Excited Molecules*; Letokhov, V. S., Ed.; Hilger: New York, 1989.

(7) Logan, D. E.; Wolynes, P. G. *J. Chem. Phys.* **1990**, *93*, 4994.

(8) Burleigh, D.; Sibert, E. L., III. *J. Chem. Phys.* **1993**, *98*, 8419.

(9) Gruebele, M. *J. Phys. Chem.* **1996**, *100*, 12183.

(10) Clouthier, D. J.; Ramsay, D. A. *Annu. Rev. Phys. Chem.* **1983**, *34*, 31. Dai, H. L.; Korpa, C. L.; Kinsey, J. L.; Field, R. W. *J. Chem. Phys.* **1985**, *82*, 1688. Polik, W. F.; Guyer, D. R.; Moore, C. B. *Ibid.* **1990**, *92*, 3453.

(11) McCoy, A. B.; Burleigh, D. C.; Sibert, E. L., III. *J. Chem. Phys.* **1991**, *95*, 7449.

(12) Leitner, D. M.; Wolynes, P. G. *J. Chem. Phys.*, in press.

(13) Field, R. W.; Coy, S. L.; Solina, S. A. B. *Prog. Theor. Phys. Suppl.* **1994**, *116*, 143 and references therein.

(14) Leitner, D. M.; Wolynes, P. G. *Phys. Rev. Lett.* **1996**, *76*, 216.

(15) Mills, I. M. In *Molecular Spectroscopy: Modern Research*; Rao, K. N., Matthews, C. W., Eds.; Academic: New York, 1972. Whetton, N. T.; Lawrence, W. D. *J. Phys. Chem.* **1989**, *93*, 5377. Rashev, S. *Chem. Phys.* **1990**, *147*, 221.

(16) A model of the same structure has been proposed to describe a semiclassical mechanism known as dynamical tunneling in the work of Heller.[28]

(17) Madsen, D.; Gruebele, M. Submitted to *J. Chem. Phys.*

(18) Leitner, D. M.; Wolynes, P. G. *Chem. Phys. Lett.* **1996**, *258*, 18.

(19) Thouless, D. J. *Phys. Rep.* **1974**, *13*, 93.

(20) Stewart, G. M.; McDonald, J. D. *J. Chem. Phys.* **1983**, *78*, 3907.

(21) Perry, D. S. *J. Chem. Phys.* **1993**, *98*, 6665. Bethardy, G. A.; Perry, D. S. *J. Chem. Phys.* **1993**, *99*, 9400. Go, J.; Perry, D. S. *J. Chem. Phys.* **1995**, *103*, 5194.

(22) Bigwood, R.; Gruebele, M. *ACH Models in Chemsitry—Symposium in Print*, in press.

(23) Stuchebrukhov, A. A. *Sov. Phys. JETP* **1986**, *64*, 1195.

(24) Stone, J.; Thiele, E.; Goodman, M. F. *J. Chem. Phys.* **1981**, *75*, 1712.

(25) Schofield, S. A.; Wolynes, P. G. *J. Chem. Phys.* **1993**, *98*, 1123. Schofield, S. A.; Wolynes, P. G. *J. Phys. Chem.* **1995**, *99*, 2753.

(26) Schofield, S. A.; Wolynes, P. G.; Wyatt, R. E. *Phys. Rev. Lett.* **1995**, *74*, 3720. Schofield, S. A.; Wyatt, R. E.; Wolynes, P. G. *J. Chem. Phys.* **1996**, *105*, 940.

(27) Logan, D. E.; Wolynes, P. G. *J. Chem. Phys.* **1986**, *85*, 937.

(28) Heller, E. J. *J. Phys. Chem.* **1995**, *99*, 2625.

(29) Go, J.; Cronin, T. J.; Perry, D. S. *Chem. Phys.* **1993**, *175*, 127. Bethardy, G. A.; Wang, X.; Perry, D. S. *Can. J. Chem.* **1994**, *72*, 652.

(30) Realistic values of σ lie in the range 3−10.[4] We use $\sigma = 10$ for formaldehyde, but note that smaller σ slightly increases T, lowering slightly predictions for $\langle y \rangle$. For example, when $\sigma = 3$ we find $T = 0.47$ and $\langle y \rangle = 0.20$ at $N_t = 8$.

(31) McIlroy, A.; Nesbitt, D. J.; Kerstel, E. R. Th.; Lehmann, K. K.; Pate, B. H.; Scoles, G. *J. Chem. Phys.* **1994**, *100*, 2596.

(32) Gambogi, J. E.; Kerstel, E. R. Th.; Lehmann, K. K.; Scoles, G. *J. Chem. Phys.* **1994**, *100*, 2612.

(33) Mehta, A.; Stuchebrukhov, A. A.; Marcus, R. A. *J. Phys. Chem.* **1995**, *99*, 2677.

(34) Kellman, M. *J. Chem. Phys.* **1985**, *83*, 3843. Kellman, M.; Xiao, L. *Chem. Phys. Lett.* **1989**, *162*, 486.

(35) Gambogi, J. E.; Timmermans, J. H.; Lehmann,K. K.; Scoles, G. *J. Chem. Phys.* **1993**, *99*, 9314.

(36) See section II of ref 7.